Structure-Based Design of Potent and Selective CK1γ Inhibitors
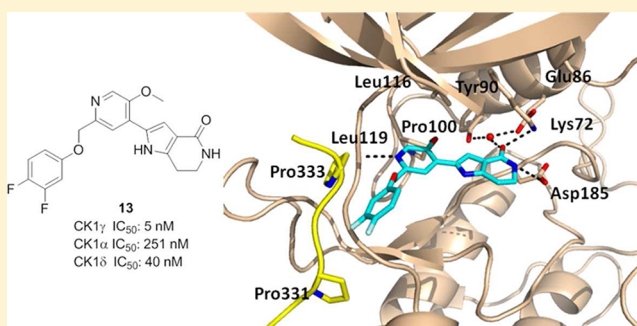
Hongbing Huang,*[†] Lisa Acquaviva,[§] Virginia Berry,[‡] Howard Bregman,[†] Nagasree Chakka,[†] Anne O'Connor,[ǁ] Erin F. DiMauro,[†] Jennifer Dovey,[§] Oleg Epstein,[†] Barbara Grubinska,[§] Jon Goldstein,[§] Hakan Gunaydin,[ǁ] Zihao Hua,[†] Xin Huang,[ǁ] Liyue Huang,[‡] Jason Human,[†] Alex Long,[ǁ] John Newcomb,[§] Vinod F. Patel,[†,⊥] Doug Saffran,[§] Randy Serafino,[§] Steve Schneider,[ǁ] Craig Strathdee,[§] Jin Tang,[ǁ] Susan Turci,[§] Ryan White,[†] Violeta Yu,[ǁ] Huilin Zhao,[ǁ] Cindy Wilson,[§] and Matthew W. Martin[†]

Departments of [†]Medicinal Chemistry; [‡]Pharmacokinetics and Drug Metabolism; [§]Oncology Research; and [ǁ]Molecular Structure, Amgen Inc., 360 Binney Street, Cambridge, Massachusetts 02142, United States

Ⓢ *Supporting Information*

ABSTRACT: Aberrant activation of the Wnt pathway is believed to drive the development and growth of some cancers. The central role of CK1γ in Wnt signal transduction makes it an attractive target for the treatment of Wnt-pathway dependent cancers. We describe a structure-based approach that led to the discovery of a series of pyridyl pyrrolopyridinones as potent and selective CK1γ inhibitors. These compounds exhibited good enzyme and cell potency, as well as selectivity against other CK1 isoforms. A single oral dose of compound **13** resulted in significant inhibition of LRP6 phosphorylation in a mouse tumor PD model.

13
CK1γ IC₅₀: 5 nM
CK1α IC₅₀: 251 nM
CK1δ IC₅₀: 40 nM

KEYWORDS: *Wnt pathway, CK1γ, cancer, pyridyl pyrrolopyridinone*

The canonical Wnt pathway regulates the ability of the β-catenin protein to activate specific target genes.[1] The level of the transcriptional activator β-catenin is tightly controlled by a destruction complex, which consists of adenomatous polyposis coli (APC), Axin, casein kinase 1α (CK1α), and glycogen synthase kinase 3β (GSK3β).[2] In the absence of a Wnt signal, the Axin and APC proteins form a scaffold that facilitates the sequential phosphorylation of β-catenin by CK1α and GSK3β. These events lead to ubiquitination and ultimately degradation of β-catenin in the proteasome. Interaction of a Wnt ligand with specific receptor complexes containing a Frizzled (Fzd) family member and LDL receptor-related proteins 5 and 6 (LRP5/6) coreceptor triggers the phosphorylation of the cytoplasmic tail of LRP 5/6 proteins by CK1γ, which creates high-affinity binding sites for Axin and facilitates relocation of Axin to the cell membrane. Recruitment of the low abundance Axin protein to the cell membrane disrupts the destruction complex and leads to the accumulation and nuclear translocation of β-catenin and to subsequent activation of Wnt target genes including c-MYC,[3] Cyclin D1,[4,5] and survivin.[6,7] The central role of CK1γ in Wnt signal transduction makes it an attractive target for the treatment of Wnt-pathway dependent cancers.[8−10]

The casein kinase 1 (CK1) family of serine/threonine protein kinases is highly conserved and includes six human isoforms α, γ1, γ2, γ3, δ, and ε.[11] The CK1 proteins have the highest degree of homology in their kinase domains but differ substantially in the length and amino acid sequence of their N- and C-terminal extensions. Multiple members of the CK1 family are shown to regulate the Wnt pathway through interactions with various proteins.[12,13] For instance, phosphorylation of Ser45 in β-catenin by CK1α is an obligate priming for subsequent phosphorylation by GSK3β, which is a key step leading to β-catenin degradation.[14,15] Additionally, phosphorylation of APC by CK1δ/ε alters its binding affinity with β-catenin and regulates the assembly of the destruction complex. Because of complex positive and negative regulation of the Wnt pathway by CK1 family members, we sought to pursue CK1γ inhibitors with selectivity over other CK1 isoforms.[16] Given the role of GSK3β in regulating β-catenin, selectivity over GSK3β was also deemed important. To date, there are no reports of selective CK1γ inhibitors that demonstrate good cellular activity.[16]

The compounds presented in this study were examined for their ability to inhibit the activity of CK1 kinases (α, δ, and γ) using enzyme assays with recombinant CK1 kinase catalytic domains. Two cellular assays were developed to aid evaluation of CK1γ inhibitors. First, a proximal PO₄-LRP6 cellular assay was used to measure the inhibition of CK1γ-mediated phosphorylation of LRP6 in HEK293 cells. Second, a transcriptional Wnt reporter assay driven by multimerized TCF binding sites in the RKO colon cell line (RKO-STF) was
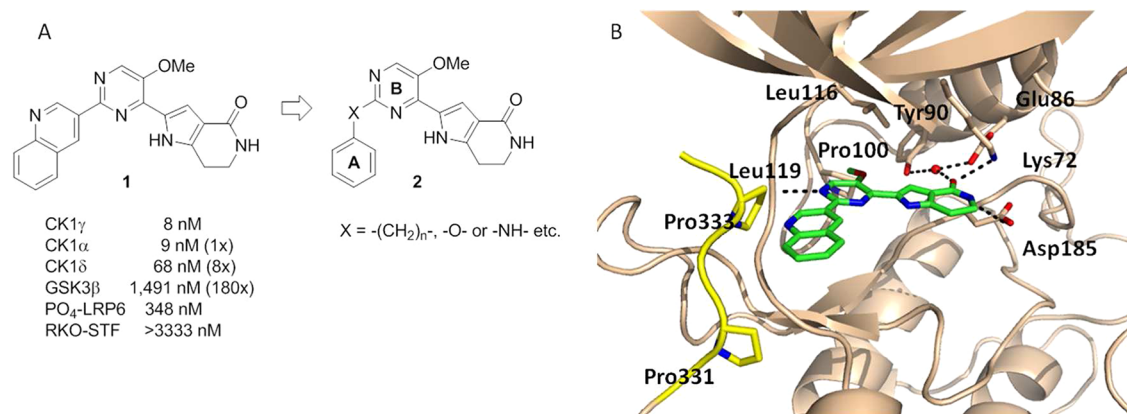
Figure 1. (A) Structure and activity of compound **1**. (B) Cocrystal structure of CK1γ complexed with **1**. The C-terminal insertion of CK1-γ is colored yellow.

Table 1. SAR of Pyrimidinyl Pyrrolopyridinones

Compd	R	CK1γ IC$_{50}$ (μM)[a]	CK1α IC$_{50}$ (μM)[a]	CK1δ IC$_{50}$ (μM)[a]	GSK3β IC$_{50}$ (μM)[a]
3	F—⟨⟩—CH=CH—	0.005	0.033	0.015	1.22
4	F—⟨⟩—CH2CH2—	0.017	0.568	0.112	25.6
5	⟨⟩—CH2—HN—	0.033	0.019	0.022	0.098
6	⟨⟩—NH—	0.008	0.054	0.022	0.016
7	F—⟨⟩—CH2—O—	0.08	0.095	0.168	> 30
8	⟨⟩—O—	0.853	18.5	4.86	> 62.5
9	F—⟨⟩—O—CH2—	0.024	0.146	0.058	1.12

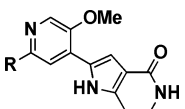[a]Values represent the mean of at least of two experiments.

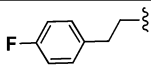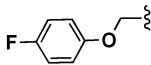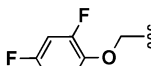employed to assess the effect of CK1γ inhibition on downstream Wnt signaling events.
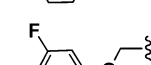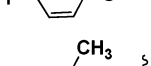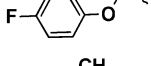
Starting from HTS hits, pyrimidinyl pyrrolopyridinone (**1**) was identified as a potent pan-CK1 inhibitor with modest selectivity over GSK3β. In enzyme assays, it was equally potent on CK1α and CK1γ and slightly less potent on CK1δ (Figure 1A). Compound **1** also exhibited robust cellular activity as measured by inhibition of PO4-LPR6. However, it was much less potent in the RKO-STF assay, which reflects its weak ability to inhibit the downstream transcription. We hypothesized that the disconnection between the two cellular assays may be due to inhibition of other CK1 isoforms acting downstream of LRP5/6. To aid the design of selective inhibitors, a cocrystal structure of **1** with CK1γ protein was obtained at 2.3 Å. The cocrystal structure reveals several key interactions between the inhibitor and the protein (Figure 1B.). The N1 of the pyrimidine core is hydrogen bonded to the

Leu119 in the hinge region of the kinase. The methoxy group is in close contact with Pro100 and the gatekeeper Leu116. The pyrrolopyridinone ring interacts with the protein through direct hydrogen bonds or through water-bridged hydrogen bond networks. The NH of the pyridinone is within the hydrogen bonding distance of Asp185, while the carbonyl group of the pyridinone directly interacts with Lys72 and engages in water-mediated hydrogen bond interactions with Glu86 and Tyr90. Intriguingly, the quinoline ring points toward the C-terminal extension that contains Pro331 and Pro333, which is unique to the CK1γ protein.[17] Because of the low homology among CK1 isoforms in their C-terminal tails, we hypothesized that interactions of small molecules with the C-terminal extension could provide the basis for selectivity over other CK1 isoforms and even greater selectivity over other kinases.[18]

We postulated that modifying the rigid bicyclic quinoline to a more flexible side chain with general structure **2** might provide

Table 2. SAR of Pyridyl Pyrrolopyridinones

Compd	R	CK1γ IC$_{50}$ (μM)[a]	CK1α IC$_{50}$ (μM)[a]	fold	CK1δ IC$_{50}$ (μM)[a]	fold	GSK3β IC$_{50}$ (μM)[a]	PO$_4$-LRP6 IC$_{50}$ (μM)[a,b]	RKO-STF IC$_{50}$ (μM)[a]
10	F—C$_6$H$_4$—CH$_2$CH$_2$—	0.026	0.736	28	0.202	8	> 62.5	0.84	1.30
11	F—C$_6$H$_4$—O—CH$_2$—	0.005	0.174	35	0.021	4	7.83	ND	0.584
12	2,4-difluorophenoxymethyl	0.003	0.225	75	0.036	12	4.00	ND	0.394
13	3,4-difluorophenoxymethyl	0.005	0.251	50	0.040	8	10.8	0.20	0.254
14	2-fluoro-3-methylphenoxymethyl	0.003	0.442	147	0.059	20	53.3	ND	0.537
15	3,4-difluoro-2-methylphenoxymethyl	0.004	0.383	96	0.114	29	38.1	0.087	0.044

[a]Values represent the mean of at least of two experiments. [b]ND = not determined.

a platform for discovery of compounds that could induce interactions with the C-terminal extension of CK1γ protein (Figure 1A). Also, varying the linkage between the pyrimidine ring and the A-ring would allow access to compounds with different dihedral angles between the two aromatic rings. Thus, a focused library of compounds with various linkers on the left-hand side of the molecule was prepared. Selected results are summarized in Table 1. In general, potency against CK1γ was not impacted significantly by these changes. A wide range of linkers showed similar potency on CK1γ with the exception of compound 8. The isoform selectivity against other CK1 enzymes, however, was influenced by the nature of the linker. For instance, 4-fluorostyryl pyrimidine (3) showed low selectivity against CK1α (7-fold) and CK1δ (3-fold). A close analog with a saturated linkage, 4-fluorophenethyl pyrimidine (4), exhibited improved selectivity against both CK1α and CK1δ (30-fold and 7-fold, respectively), albeit at the expense of potency. It was also noted that compounds having an NH group connected to the pyrimidine core, such as compounds 5 and 6, showed undesired inhibitory activity on GSK3β.

To further improve isoform selectivity, we then investigated structural modification of the central heteroaromatic B-ring. The fact that only the N1 of the pyrimidine ring of 1 was shown to make a critical hydrogen bond interaction with CK1γ protein in the cocrystal structure prompted us to investigate whether a pyridine ring could induce conformational changes that could improve isoform selectivity. This line of investigation led to the discovery of a series of pyridyl pyrrolopyridinones that were very potent on CK1γ and highly selective against other CK1 isoforms. The results are summarized in Table 2. For compounds with a two-methylene linkage between the A-ring and the central B-ring, the change from a pyrimidine to a

pyridine had no effect on either potency or selectivity. For instance, 2-(4-fluorophenethyl)pyridine (10) showed similar CK1γ potency and isoform selectivity to its pyrimidine congener 4. The pyridine ring, however, in combination with a —CH$_2$O— linkage provided compounds with improved potency and isoform selectivity. For example, 2-(4-fluorophenoxymethyl)pyridine (11) (CK1γ IC$_{50}$ 0.005 μM and CK1α selectivity 35-fold) was significantly more potent and selective against CK1α compared to its pyrimidine counterpart 9 (CK1γ IC$_{50}$ 0.024 μM and CK1α selectivity 6-fold). Intrigued by the improved isoform selectivity, further investigations were conducted on 2-phenoxymethyl pyridine by modification of the phenyl ring.

It was found that both CK1γ potency and isoform selectivity were affected by substituents. Ortho-substitution on the phenyl ring enhanced isoform selectivity, as 2-((2,4-difluorophenoxy)-methyl)pyridine (12) was considerably more selective against both CK1α and CK1δ (75-fold and 12-fold, respectively). Increase in the size of the substituent led to more selective compound 2-((2-fluoro-3-methylphenoxy)methyl)pyridine (14). Meta-substitution improved both isoform selectivity and cellular potency. For instance, 2-((3,4-difluorophenoxy)-methyl)pyridine (13) exhibited better selectivity against both CK1α and CK1δ (50-fold and 8-fold, respectively) and superior potency in the RKO-STF cell assay (IC$_{50}$ 0.254 μM). Importantly, these substitution effects appear to be additive, as a combination of ortho- and meta-substitutions led to 2-((3,4-difluoro-2-methylphenoxy)methyl)-pyridine (15), which demonstrated excellent cellular potency and was one of the most selective CK1γ inhibitors. In addition, both 13 and 15 demonstrated good kinase selectivity against a broad panel of kinases (Ambit KINOMEscan).[19]
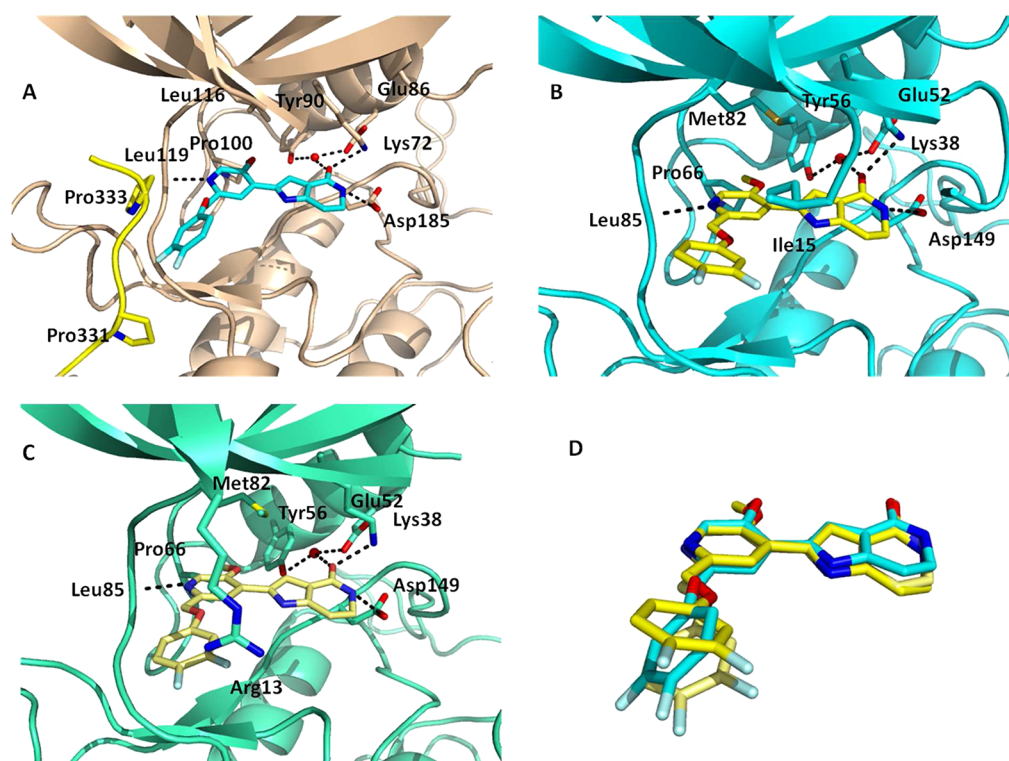
Figure 2. X-ray cocrystal structures. (A) **13** bound to CK1γ protein. The C-terminal insertion of CK1γ is colored yellow. (B) **13** bound to CK1δ protein. (C) **13** bound to CK1δ protein. (D) Overlay of different conformations of **13** as bound to CK1γ and CK1δ.

Table 3. Pharmacokinetic Parameters of Compounds 13 and 15

| | μL/(min·mg)[a] | | | | mouse po PK[e] | | | | |
compd	RLM	HLM	rPPB[b,c]	mPPB[d]	dose[f] (mg/kg)	C_{max} (μM)	$t_{1/2}$ (h)	T_{max} (h)	AUC (μM·h)
13	46	59	96.9%	95.1%	30	9.72	2.7	0.33	15.4
15	106	177	ND	99.2%	30	0.56	1.4	1.17	2.1

[a]Compounds were incubated with microsomes for 30 min at a concentration of 1 μM. [b]rPPB = rat plasma protein binding. [c]ND = not determined. [d]mPPB = mouse plasma protein binding. [e]Pharmacokinetic parameters following administration of compound **13** or **15** in male Mouse_CD1:3 animals per study. [f]Dosed in 10.0%Pluronic F68_30.0%HPBCD_60.0%water/MSA_pH2.5.

To understand the structural basis for the selectivity observed with these CK1γ inhibitors, cocrystal structures of compound **13** with CK1γ and CK1δ were obtained. The structures were resolved at 2.4 and 1.8 Å, respectively (Figure 2). Not surprisingly, compound **13** binds very similarly to the two proteins in the ATP binding pocket, as it is highly conserved among CK1 proteins. The pyrrolopyridinone moiety of **13** in both CK1γ and CK1δ cocrystal structures engages the same hydrogen bond interactions in the ATP binding pocket as compound **1**, and as a result it adopts almost identical conformations in both crystal structures. In the hinge region, the pyridyl nitrogen atom of **13** hydrogen bonds to a leucine residue, Leu119 in CK1γ and Leu116 in CK1δ, respectively. The methoxy group of **13** engages in a very similar hydrophobic interaction with the gatekeeper residues in both structures: Leu85 in CK1γ and Met 82 in CK1δ. The significant conformational difference was observed in the phenoxy-methylene moiety of **13**. In the CK1γ cocrystal structure (Figure 2A), the difluorophenyl ring engages in a "face-to-face" interaction with Pro333 and an "edge-to-face" interaction with Pro331. Since these residues are unique to the CK1γ isoform, hydrophobic interactions with them may account for the increased CK1γ potency of **13** compared to compound **1**, as a

productive hydrophobic interaction with the Pro-rich c-terminal tail was not observed in the cocrystal structure of **1** with the CK1γ protein.

There are two different conformations of the difluoro phenyl ring of **13** present in the CK1δ/**13** cocrystal structure (Figure 2B and 2C), where the c-terminal tail unique to CK1γ is absent. The difluorophenyl ring of **13** is rotated by ~60° in the CK1δ/**13** complex, and the *meta*-fluorine is flipped compared with that in the CK1γ/**13** complex. In one conformation, the difluorophenyl ring engages in hydrophobic interactions with the side chain of Ile15 from the glycine rich loop and the *meta*-F atom points to the solvent front (Figure 2B). In the other conformation, the *meta*-F atom of the difluoro phenyl ring hydrogen bonds to Arg13 (Figure 2C). The CK1δ/**13** cocrystal structure suggests that compound **15** will have to adopt different conformations in binding with the CK1δ protein than compound **13**, because the methyl group at the 2-position of the phenyl ring in **15** would bump into the hinge region of the protein if it binds the same way as **13**. Consequently, in the absence of the favorable interactions of the phenyl ring with the protein observed in the CK1δ/**13** complex, compound **15** is expected to bind to the CK1δ protein less favorably than **13**. This may explain the significant loss of CK1δ potency of **15**.

In light of their excellent enzyme and cellular potencies, compounds **13** and **15** were evaluated in vivo in pharmacokinetic (PK) studies in rodents. The key PK parameters of compounds **13** and **15** are summarized in Table 3. Compound **13** demonstrated low turnover in human and rat liver microsomes. It provided a reasonable plasma exposure when dosed orally in mice at 30 mg/kg. On the other hand, compound **15** exhibited high intrinsic clearance in human and rat liver microsomes and demonstrated low oral exposure in mice at 30 mg/kg. The ortho-methyl group may account for the higher intrinsic clearance, as compound **14** also exhibited similarly high turnover in human and rat liver microsomes [HLM/RLM 123/88 μL/(min·mg)].

Compound **13** was then evaluated in a pharmacodynamic (PD) assay measuring the inhibition of CK1γ-mediated LRP6 phosphorylation in a human tumor xenograft mouse model. Subcutaneous tumors were formed in athymic nude mice using a HEK293 cell line that constitutively expressed LPR6 and had doxycycline-inducible expression of CK1γ. Mice were treated for 24 h with doxycycline (DOX, 0.5 mg/mL) in the drinking water to stimulate LRP6 phosphorylation before compound **13** was dosed orally at 50 mg/kg. The tumor tissues and plasma were collected 6 h postdosing, and LRP6 phosphorylation levels were quantified by an electrochemiluminescent assay. Significant inhibition (42%) of LRP6 phosphorylation was observed with an associated plasma exposure of **13** of approximately 2.7 μM (Figure 3) and a plasma unbound concentration of **13** at 0.13 μM, which is consistent with its PO$_4$-LRP6 cellular potency (IC$_{50}$ 0.20 μM, Table 2).
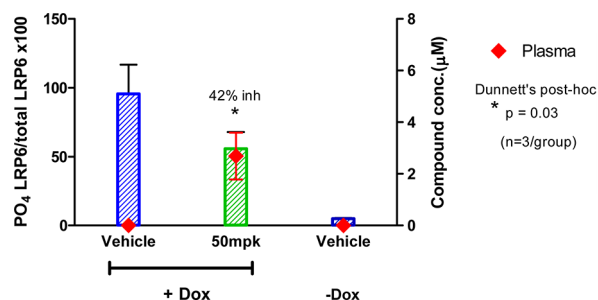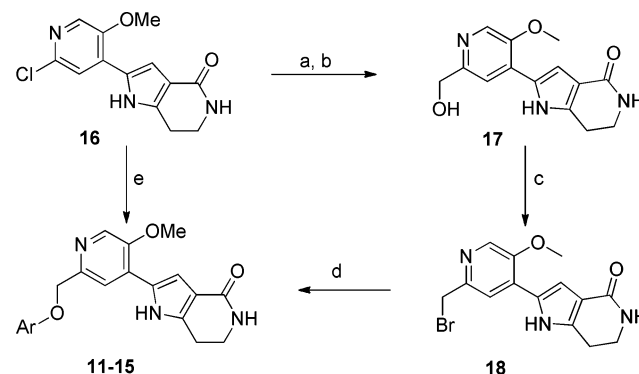

Figure 3. Effect of compound **13** on CK1γ-mediated LRP6 phosphorylation in the human tumor xenograft model.

Compounds **11**−**15** were synthesized according to the routes outlined in Scheme 1. The synthesis commenced with carbonylation of pyridyl pyrrolopyridinone **16**. The resulting methyl ester was reduced to primary alcohol **17**, which was subsequently converted to corresponding bromide **18**.[20] Nucleophilic substitution of **18** with phenols led to compounds **11**−**14**. Alternatively, a Suzuki coupling of **16** with the corresponding boronic ester furnished **15**.

We have described the design, synthesis, and biological evaluation of a novel series of pyridyl pyrrolopyridinones as selective CK1γ inhibitors. Compound **13** demonstrated excellent CK1γ potency in both enzyme and cell assays, and it exhibited good selectivity against other CK1 isoforms. X-ray cocrystal structures revealed significantly different binding conformations of **13** in CK1γ and CK1δ proteins. The binding-mode differences were used to formulate a general hypothesis for the observed selectivity of this series of inhibitors. A single dose of compound **13** resulted in significant inhibition of LRP6 phosphorylation in a mouse tumor PD

Scheme 1. Synthesis of Compounds 11−15[a]

[a]Reagents: (a) CO, Et$_3$N, PdCl$_2$dppf, MeOH, 95 °C; (b) DIBAL-H, DCM, 65%; (c) SOBr$_2$, DMF, 45%; (d) ArOH, K$_2$CO$_3$, DMF. (e) 2-((4,5-difluoro-2-methylphenoxy)methyl)-4,4,5,5-tetramethyl-1,3,2-dioxaborolane, PdCl$_2$AmPhos, K$_2$CO$_3$, dioxane, 120 °C; 40%.

model. Further investigations into the effects of selective pharmacological inhibition of CK1γ in disease relevant models will be disclosed in future communications.

ASSOCIATED CONTENT

Ⓢ Supporting Information
Experimental details, synthesis of compound **16**, biological assays, kinase selectivity, and X-ray crytstallographic information. This material is available free of charge via the Internet at http://pubs.acs.org.

Accession Codes
The PDB accession codes for the X-ray cocrystal structures of CK1γ + **1**, CK1γ + **13**, and CK1δ + **13** are 4HGL, 4HGS, and 4HGT, respectively.

AUTHOR INFORMATION

Corresponding Author
*Tel: 617-444-5197. E-mail: hongbing.huang@amgen.com.

Present Address
⊥Sanofi-Aventis, 270 Albany Street, Cambridge, Massachusetts 02139.

Notes
The authors declare no competing financial interest.

ABBREVIATIONS

APC, adenomatous polyposis coli; CK1, casein-kinase 1; GSK3β, glycogen synthase kinase 3β; LRP5/6, LDL receptor-related proteins 5 and 6; PPB, plasma protein binding; STF, Super TOP-Flash

REFERENCES

(1) Gordon, M. D.; Nusse, R. Wnt signaling: multiple pathways, multiple receptors, and multiple transcription factors. *J. Biol. Chem.* **2006**, *281*, 22429−22433.

(2) Kimelman, D.; Xu, W. beta-catenin destruction complex: insights and questions from a structural perspective. *Oncogene* **2006**, *25*, 7482−7491.

(3) Yochum, G. S.; Sherrick, C. M.; Macpartlin, M.; Goodman, R. H. A beta-catenin/TCF-coordinated chromatin loop at MYC integrates 5′ and 3′ Wnt responsive enhancers. *Proc. Natl. Acad. Sci. U. S. A.* **2010**, *107*, 145−150.

(4) Mirando, A. J.; Maruyama, T.; Fu, J.; Yu, H. M.; Hsu, W. beta-catenin/cyclin D1 mediated development of suture mesenchyme in calvarial morphogenesis. *BMC Dev. Biol.* **2010**, *10*, 116.

(5) Tetsu, O.; McCormick, F. Beta-catenin regulates expression of cyclin D1 in colon carcinoma cells. *Nature* **1999**, *398*, 422−426.

(6) Ma, H.; Nguyen, C.; Lee, K. S.; Kahn, M. Differential roles for the coactivators CBP and p300 on TCF/beta-catenin-mediated survivin gene expression. *Oncogene* **2005**, *24*, 3619−3631.

(7) Kim, P. J.; Plescia, J.; Clevers, H.; Fearon, E. R.; Altieri, D. C. Survivin and molecular pathogenesis of colorectal cancer. *Lancet* **2003**, *362*, 205−209.

(8) Davidson, G.; Wu, W.; Shen, J.; Bilic, J.; Fenger, U.; Stannek, P.; Glinka, A.; Niehrs, C. Casein kinase 1 gamma couples Wnt receptor activation to cytoplasmic signal transduction. *Nature* **2005**, *438*, 867−872.

(9) Barker, N.; Clevers, H. Mining the Wnt pathway for cancer therapeutics. *Nat. Rev. Drug Discovery* **2006**, *5*, 997−1014.

(10) Klaus, A.; Birchmeier, W. Wnt signalling and its impact on development and cancer. *Nat. Rev. Cancer* **2008**, *8*, 387−398.

(11) Price, M. A. CKI, there's more than one: casein kinase I family members in Wnt and Hedgehog signaling. *Genes Dev.* **2006**, *20*, 399−410.

(12) McKay, R. M.; Peters, J. M.; Graff, J. M. The casein kinase I family in Wnt signaling. *Dev. Biol.* **2001**, *235*, 388−396.

(13) Thorne, C. A.; Hanson, A. J.; Schneider, J.; Tahinci, E.; Orton, D.; Cselenyi, C. S.; Jernigan, K. K.; Meyers, K. C.; Hang, B. I.; Waterson, A. G.; Kim, K.; Melancon, B.; Ghidu, V. P.; Sulikowski, G. A.; LaFleur, B.; Salic, A.; Lee, L. A.; Miller, D. M., 3rd; Lee, E. Small-molecule inhibition of Wnt signaling through activation of casein kinase 1alpha. *Nat. Chem. Biol.* **2010**, *6*, 829−836.

(14) Liu, C.; Li, Y.; Semenov, M.; Han, C.; Baeg, G. H.; Tan, Y.; Zhang, Z.; Lin, X.; He, X. Control of beta-catenin phosphorylation/degradation by a dual-kinase mechanism. *Cell* **2002**, *108*, 837−847.

(15) Amit, S.; Hatzubai, A.; Birman, Y.; Andersen, J. S.; Ben-Shushan, E.; Mann, M.; Ben-Neriah, Y.; Alkalay, I. Axin-mediated CKI phosphorylation of beta-catenin at Ser 45: a molecular switch for the Wnt pathway. *Genes Dev.* **2002**, *16*, 1066−1076.

(16) Hua, Z.; Huang, X.; Bregman, H.; Chakka, N.; Dimauro, E. F.; Doherty, E. M.; Goldstein, J.; Gunaydin, H.; Huang, H.; Mercede, S.; Newcomb, J.; Patel, V. F.; Turci, S. M.; Yan, J.; Wilson, C.; Martin, M. W. 2-Phenylamino-6-cyano-1H-benzimidazole-based isoform selective casein kinase 1 gamma (CK1gamma) inhibitors. *Bioorg. Med. Chem. Lett.* **2012**, *22*, 5392−5395.

(17) http://kinase.com/human/kinome/ (accessed June 2012).

(18) Long, A.; Zhao, H.; Huang, X. Structural basis for the interaction between casein kinase 1 delta and a potent and selective inhibitor. *J. Med. Chem.* **2012**, *55*, 956−960.

(19) See the Supporting Information for details.

(20) Nagle, A. S. S., R. N.; Chong, B. D.; Jung, K. W. Efficient synthesis of *β*-amino bromides. *Tetrahedron Lett.* **2000**, *41*, 3011−3014.